Prediction of porosity of food materials during drying: Current challenges and future directions

Mohammad U. H. Joardder, C. Kumar & M. A. Karim

Prediction of porosity of food materials during drying: Current challenges and future directions

Mohammad U. H. Joardder,a,b C. Kumar,a and M. A. Karima

aFaculty of Engineering and Science, Queensland University of Technology, Brisbane, Queensland 4001, Australia

bDepartment of Mechanical Engineering, Rajshahi University of Engineering and Technology, Bangladesh

muhjoardder@gmail.com,

chandan.kumar@hdr.qut.edu.au,

azharul.karim@qut.edu.au,

Corresponding author: M.U.H Joardder Tel+8801734815621, Email: muhjoardder@gmail.com

Abstract

Pore formation in food samples is a common physical phenomenon observed during dehydration processes. The pore evolution during drying significantly affects the physical properties and quality of dried foods. Therefore, it should be taken into consideration when predicting transport processes in the drying sample. Characteristics of pore formation depend on the drying process parameters, product properties and processing time. Understanding the physics of pore formation and evolution during drying will assist in accurately predicting the drying kinetics and quality of food materials. Researchers have been trying to develop mathematical models to describe the pore formation and evolution during drying. In this study, existing porosity models are critically analysed and limitations are identified. Better insight into the factors affecting porosity is provided, and suggestions are proposed to overcome the limitations. These include considerations of process parameters such as glass transition temperature, sample temperature, and variable material properties in the porosity models. Several researchers have proposed models for porosity prediction of food materials during drying. However, these models are either very simplistic or empirical in nature and failed to consider relevant significant factors that influence porosity.

In-depth understanding of characteristics of the pore is required for developing a generic model of porosity. A micro-level analysis of pore formation is presented for better understanding, which will help in developing an accurate and generic porosity model.

Keywords

Pore formation, drying conditions, food properties, porosity prediction models, microstructure

1 Introduction

Food is one of the complex varieties of soft matter due to its heterogeneous hierarchical structure (de Kruif, 2012; van der Sman & van der Goot, 2009). The porous structure of plant-based materials is a dominant factor that significantly affects the heat and mass transfer phenomena, as well as quality characteristics during drying (Del Valle, Cuadros, & Aguilera, 1998; Karathanos, Kanellopoulos, & Belessiotis, 1996b; Liu, 2010; Marousis & Saravacos, 1990; Xiong, Narsimhan, & Okos, 1992). Moreover, pore formation has a positive influence on the quality attributes of dried food. In addition to this, the diffusivity of the gaseous phase was found as directly proportional to the porosity of the food materials (Karathanos, Anglea, & Karel, 1993). Therefore, the understanding fundamental process of pore formation and evolution may assist in the prediction of drying kinetics and in the modelling of drying of food materials (Karathanos et al., 1996b; Karunasena, Senadeera, Brown, & Gu, 2014).

Drying methods and conditions influence the porosity of the final dried product. Thus, the same raw material may end up with different pore characteristics based on the drying process (Sablani et al., 2007). Porosity also has a direct effect on other physical properties such as mass diffusion coefficient, thermal conductivity and thermal diffusivity (Joardder, Kumar, & Karim, 2017a; Rahman, 2001). In contrast, collapse and shrinkage negatively affect the volatility of fluids, rehydration capacity and rehydration rate (Karathanos et al., 1993). Mechanical and textural properties of food are also correlated to the porosity. For example, Vincent (1989) found that the torsional stiffness (0.5–7 MPa) varied with the porosity (0.83–0.54) in apple samples.

Porosity plays the most important role in the overall strength of dried foods. The porosity also gives an indication of the extent of shrinkage in the food material undergoing drying, which in turn determines the size and shape of the finished product (Ayrosa & Pitombo, 2003). This knowledge of the porous structure of the dehydrated materials will help in the modelling of heat

and mass transfer and may also assist in designing an efficient drying system (Bai, Rahman, Perera, Smith, & Melton, 2001; Datta, 2007; Karathanos et al., 1996b).

Several mathematical models have been proposed to predict the porosity of a material as a function of the moisture content. These models can be grouped into two categories: (i) theoretical models which are based on the understanding of the fundamental phenomena and mechanisms that may be involved in pore formation, and (ii) empirical models which are based on fitting the model parameters to the experimental data. Most of the studies predicted porosity by empirical correlations as a function of water content in the form of linear (Bhatnagar & Hanna, 1997), quadratic (Hutchinson, Siodlak, & Smith, 1987), exponential (Huang & Clayton, 1990) and power law equations (Madamba, Driscoll, & Buckle, 1994; Rapusas & Driscoll, 1995). Even though the empirical models give a reasonable prediction, they offer limited insight into the fundamental principles involved, limiting the understanding of the mechanisms responsible for water removal.

The first theoretical porosity model was published in the 1950s when Kilpatric, Lowe and Van Arsdel (1955) developed a simple model considering the volumetric shrinkage of fruits and vegetables during drying. Most of the theoretical predictions are based on the conservation of mass and volume principle. Ideal shrinkage assumes the volume reduction of the product is exactly equal to the volume of the removed water during drying. However, no food product entirely follows the ideal shrinkage rule. In reality, the shrinkage depends on many factors including the material properties, drying conditions and processing time. In addition to this, there is no model available in the literature that considers the transport phenomena of bound water separately. Consideration of both bound water and free water along with other phases such as water vapour and the air is essential to get a better understanding of porosity development and shrinkage.

This study presents a critical discussion of the models for pore formation in foods during drying. Both empirical and theoretical models available in the literature have been discussed

extensively. Some recommendations are made to overcome the limitations of the existing models and to develop a comprehensive theoretical model for porosity prediction.

2 Models of Porosity

The models are usually classified as empirical and theoretical models. Empirical models are developed by analysing experimental data, and the theoretical models are based on the physical interpretation of the structure of food materials. This section critically analyses both types of models.Before being critical, the definitions of porosity related terms are presented in the following section.

2.1 Definition of the terms used

The variables relevant to porosity models need to be defined to assist in understanding the physical significance of these models (Krokida, Zogzas, & Maroulis, 1997; Rahman, Perera, Chen, Driscoll, & Potluri, 1996; Santos & Silva, 2008; Shafiur Rahman, 2003; Zogzas, Maroulis, & Marinos-Kouris, 1994).

Moisture content

Based on the reference mass of the sample, moisture content can be expressed as dry basis as well as a wet basis. The moisture content on a dry basis can be calculated by equation (1),

$$X = \frac{m_w}{m_s} \quad (1)$$

Moreover, the moisture content on the wet basis can be expressed as:

$$w = \frac{X}{1+X} \quad (2)$$

Substance density (ρ_s)

The substance density is the density of solid material in a sample. This density is also regarded as material density (ρ_m) in some literature and can be expressed as:

$$\rho_m = \rho_s = \frac{m_s}{V_s} \quad (3)$$

Particle density (ρ_p)

This is defined as the density of a sample excluding all the open and closed pores, as expressed in equation (4):

$$\rho_p = \frac{m_s + m_w}{V_s + V_w} = \frac{1 + X}{\dfrac{1}{\rho_s} + \dfrac{X}{\rho_w}} \quad (4)$$

Bulk density

Bulk density can be obtained as a function of moisture and volume, and expressed as follows,

$$\rho_b = \frac{m_s + m_w}{V_s + V_w + V_a} \quad (5)$$

Porosity (ε)

Food material is a combination of solid, liquid and gas. The porosity is defined as the fraction of the void volume of air in the total volume. It can be obtained from the following relationship:

$$\varepsilon = \frac{V_a}{V_s + V_w + V_a} = 1 - \frac{V_s + V_w}{V} \quad (6)$$

Porosity can also be estimated from the apparent density, and the true density of the material and thus can also be expressed by the following equation:

$$\varepsilon = 1 - \frac{\rho_b}{\rho_p} \quad (7) \text{ss}$$

Initial porosity (ε_0)

All plant-based materials contain some void spaces in their fresh state. This void space is known as initial porosity and can be expressed by the following equation:

$$\varepsilon = 1 - \frac{\rho_{b0}}{\rho_{p0}} = 1 - \frac{V_s + V_w}{V_0} \quad (8)$$

2.2 Empirical models

Empirical models are developed using experimental data to fit parameters for a particular process. Methods, materials and the processing environment limit these models, and the fitting parameters usually have no physical significance. Despite the existence of these limitations, the empirical models are beneficial to a certain extent. Table 1 presents the selected empirical models for porosity developed in the last three decades for different types of food materials. Values of coefficients a, b and c in various models are different due to the differences in experimental conditions. All the empirical models presented in Table 1 were developed by correlating the moisture content of the sample with porosity.

It was found that the proposed relationships strongly agree with the experimental data. Alongside linear relationships between moisture content and porosity, other trends like exponential and power relationships were also observed. For example, Modamba et al. (1994), Lozano et al.(1980) and Rapusas et al. (1995) expressed porosity using quadratic, exponential and power law equations respectively. These models have a higher accuracy of prediction but are only applicable to the specific products and processes. Thus, they cannot be used for diversified products and processes or as a tool for prediction because slight changes of process conditions and sample parameters significantly alter the value of fitting parameters.

2.3 Semi-empirical models

The semi-empirical models are not completely based on experimental data fitting. These models are theoretical models but are highly dependent on the experimental results for some parameters.

2.3.1 Porosity determination from shrinkage curves

As mentioned above, ideal shrinkage is observed when the volume reduction of the product is exactly equal to the volume of the removed water during drying. If this occurs, it is assumed that there is a change in the porosity of the product, without the development of new pores.

Conversely, when the volume reduction is smaller than the volume of removed water, this means that new pores are formed during drying. There are several mathematical models available in the literature that relate shrinkage and porosity. It is also possible to determine the porosity during drying from the graphical representation of the mathematical expression of shrinkage. Madiouli et al. [33] have developed a graphical method for measuring porosity from a shrinkage curve, as shown in Figure 1. The figure presents an experimental shrinkage curve, an ideal shrinkage biased curve, and an ideal shrinkage curve. The authors proposed that porosity can be calculated from the ratio of experimental points (z) to the deviations of experimental points from the ideal value (y).

Therefore, the porosity is expressed as:

$$\varepsilon = \frac{AD}{AC} = \frac{z - y(1 - \varepsilon_0)}{z} \quad (9)$$

This model is one of the empirical models that relates porosity directly with shrinkage. Another model developed by Katekawa et al. (2004) offers a general relationship between shrinkage and porosity. That model took into account some variables including the initial density of the wet product, true density of the liquid phase and true density of the solid phase. From that study, it was found that the ratio of initial and final solid volume $\frac{(1 - \varepsilon)V}{(1 - \varepsilon_0)V_0}$ varied linearly with the amount of mass reduction expressed as $\frac{X}{X_0}$. From this relationship, shrinkage and porosity can be correlated by the following equation.

$$\frac{1 - \varepsilon}{1 - \varepsilon_0} = \frac{1}{\left(\frac{\rho_s}{\rho_w}\right)X + 1}\left[1 + X\left(\frac{X}{X_0}\frac{\rho_s}{\rho_w}\right)\right]\frac{V}{V_0} \quad (10)$$

Another model proposed by Perez and Calvelo (1984), as shown in equation (11), provides a good fit for experimental data. If shrinkage data is available, the porosity of the sample can be obtained easily using the equation.

$$\frac{V}{V_0} = \frac{1}{1-\varepsilon}\left[1 + \frac{\rho_s\left(X - X_0\right)}{\left(1 + X_0\right)} - \varepsilon_0\right] (11)$$

These shrinkage-based models offer a good fit to the experimental data. However, due to the necessity of experimental shrinkage data, these are categorised as empirical models.

2.3.2 Porosity prediction using a hybrid neural network

An artificial neural network (ANN), as shown in Figure 2, is a powerful tool for modelling. When sufficient experimental data is available, ANN offers accurate and cost-effective methods of developing important relationships between the selected variables (Hussain, 1999). There are many types of ANN, including multilayer perception, recurrent neural networks, and radial basis function networks. Prediction of porosity depends on different factors like drying method, drying parameters and food types. In the literature, a significant amount of experimental data on the relationships between various variables and porosity is available. Therefore, ANN is a promising approach for the development of a porosity model. However, insufficient investigations have been reported so far in the literature.

Hussain et al. (2002) developed a generic model for the porosity prediction using a hybrid neural network. In that model, 286 datasets were used for four input variables: temperature, water content, initial porosity and type of product.

Depending on the inputs, three different models were proposed in that investigation as shown in Table 2. From Table 2, it is apparent that model based only on temperature and moisture content has a higher amount of error. However, it is clearly observed that minimum error was evident when temperature, water content, type food product and the initial porosity are taken into consideration.

Although empirical models demonstrate a high level of accuracy in predicting the porosity, these models still have the following limitations:

- They are not generic as they depend on the types of products and the drying conditions such as temperature, pressure, humidity and processing time.

- Empirical models are specially developed to fit the experimental data for particular drying conditions and material properties. Therefore, these models cannot be replicated to predict porosity for different processes and materials.

- The empirical models are purely based on experimental data with minimum consideration of the fundamental physics of the interrelation between process variables and sample properties. For this reason, a basic understanding of the physics that governs the structural change (formation of the pore) cannot be understood from the empirical models.

It is thus essential to develop theoretical models as they have better insight on the fundamental physics and therefore can be used for a broad range of processes and products.

2.4 Theoretical models of porosity

Most of the theoretical models are based on the conversion of mass and volume principle. The first theoretical porosity model was developed by Kilpatric et al. (1955). It was a simple model that considered the volumetric shrinkage of fruits and vegetables during drying. This model only considers bulk and solid density as shown in equation (12) (Miles, Beck, & & Veerkamp, 1983).

$$\varepsilon = 1 - \frac{\rho_b}{\rho_s} \quad (12)$$

Although this model has physical significance, it needs instantaneous experimental values of bulk density of the sample. Lozano et al.(1983) developed the following generalised equation to predict the porosity of foodstuffs. It assumes that a linear relationship between porosity and moisture content exists during drying and is expressed by:

$$\varepsilon = \frac{(X+1)}{(X_0+1)} \frac{\rho_{b0}}{\rho_b} \quad (13)$$

Their experimental results agreed fairly well with predicted values for garlic, sweet potato and potato, but the predicted porosity of other materials was not accurate. For example, this model completely failed to predict the porosity of carrots with various moisture contents. This inconsistency may be due to the assumption of the shrinkage phenomenon as a linear function of moisture content. In general, many of the food materials do not show the linear relationship between volume shrinkage and volume of migrated water at any time during drying (Lozano et al., 1980; Madamba et al., 1994; Rapusas & Driscoll, 1995).

In order to resolve this shrinkage and moisture content relationship, Zogzas et al. (1994), proposed a model considering the volume shrinkage coefficient (β). Three other fitting parameters, namely, density of dry solids (ρ_s), enclosed water density (ρ_w) and the bulk density of the dry solids (ρ_b) were also included in their model, as shown in equation (14).

$$\varepsilon = 1 - \frac{\rho_{b0}\left[\rho_w + X\rho_s\right]}{\rho_w\rho_s\left[1 + \beta X\right]} \quad (14)$$

Several researchers have used this model with various drying methods and different food products. A summary of such research works is presented in Table 3.

Although many researchers used this model as a general model, the prediction accuracy of this model widely varies depending on the product type and drying process. One possible reason for this is beacuse all of the parameters associated with this model are strongly dependent on the drying method and material properties (Krokida & Maroulis, 1997). The effect of process parameters and product variants on these four fitting parameters is described below:

- Dry solid density (ρ_s) is an inherent material property that is significantly affected by the type of material being studied, as it is highly dependent on material composition and structure. This value usually does not depend on normal drying conditions; however, extreme drying conditions such as high temperature may affect the value of dry solid density.

- Enclosed water density (ρ_w) is not much dependent on either drying method or material (Krokida & Maroulis, 1997).

- The bulk density of dry solids (ρ_b) is the property that is significantly affected by both material properties and process parameters. Therefore, this parameter is changed throughout the drying period and real-time measurement of this parameter is challenging and extraordinary device will be required for this purpose.

- Volume shrinkage coefficient (β) is similar in nature to bulk density and is strongly dependent on drying methods and material properties.

Shrinkage is considered as the representation of structural changes in the material observed during drying. However, Shafiur Rahman (2003) found that it cannot represent internal and external structural modification during drying. He hypothesised that capillary force is the main force that causes the collapse of tissue and the counterbalancing of this force is responsible for the formation of pores. To represent this force-balancing hypothesis, a new parameters shrinkage-expansion coefficient was introduced , and the author developed two models for the pattern of shrinkage considering ideal and non-ideal conditions.

In ideal condition, it is assumed that the volume of developed pores does not contribute to shrinkage and therefore shrinkage is equal to the volume of water removed during drying. Equation (15) was developed to calculate the apparent porosity of porous food materials.

$$\varepsilon = \varepsilon_0 + \left(1 - \varepsilon_0\right)\frac{\alpha}{\alpha + \beta'} \quad (15)$$

where the volume of formed pores due to loss of water is expressed as $\dfrac{1 - M}{\rho_w}$,

moreover, volume of solid including water is expressed as, $\beta' = \dfrac{M}{\rho_m}$.

By adding the shrinkage-expansion coefficient to the ideal model, the non-ideal model for real food materials can be obtained. The shrinkage-expansion coefficient can be calculated by considering the relationship between initial porosity, actually measured porosity and the values of α and β, as shown in equations (16) and (17).

$$\text{Shrinakge-expansion coefficient, } \varphi = \frac{\beta\left(\varepsilon_0 - \varepsilon'\right)}{\alpha\left(\varepsilon - 1\right)} \quad (16)$$

$$\text{moreover, } \varepsilon' = \frac{\varphi\alpha}{\varphi\alpha + \beta} \quad (17)$$

It can be seen in equation (16) that the shrinkage-expansion coefficient requires experimental values of initial and instantaneous porosity. Initial porosity is the material property; however, instantaneous porosity requires experimental measurement. Therefore, the main difficulty in using this particular model is the instantaneous measurement of porosity and eventually the shrinkage-expansion coefficient, ϕ as it is significantly influenced by process parameters and characteristics of food materials. As the determination of this coefficient requires experimental data, this porosity model becomes dependent on the observed value of these variables.

The author (Rahman, 2003) assumed that initial porosity ε_0 remains constant throughout the drying process although the initial air volume is severely affected when the product is under extreme heating.

However, both collapse and shrinkage take place in the food material during drying. In literature, this shrinkage refers to an overall volume reduction phenomenon; whereas, collapse represents irreversible changes of volume (Prothon, Ahrné, & Sjöholm, 2003).

In order to introduce the collapse phenomenon, Khallofi et al.(2009) took into account the possible change of volume during the drying processes. In their prediction model of porosity, both collapse function $\delta(X)$ and shrinkage function $\phi(X)$ were taken into consideration. The authors defined the collapse function as:

$$\delta(X) = \frac{V_{a/a}(X)}{V_a^0} \quad (18)$$

where, $V_{a/a}(X)$ is the evolution of air within the solid matrix.

Finally, expression for the theoretical model of porosity considering the collapse function and the shrinkage function was proposed as shown in equation (19).

$$\varepsilon(X) = \frac{A + BX}{C + DX} \quad (19)$$

where,

$$A = \varepsilon_0 \delta(X) + X_0 \beta \left[\varphi(X)(1 - \varepsilon_0) + \varepsilon_0 \delta(X) \right]$$

$$B = \beta \varphi(X)(1 - \varepsilon_0)$$

$$C = 1 - \varepsilon_0 + \varepsilon_0 \delta(X) + X_0 \beta \left[\varphi(X)(1 - \varepsilon_0) + \varepsilon_0 \delta(X) \right]$$

$$D = \beta(1 - \varepsilon_0) \left[1 - \varphi(X) \right]$$

Despite the incorporation of some physics in the above model, some critical questions can be raised:

- This model suggested use of shrinkage and/or collapse function. However, no clear guidelines for using these functions were outlined.

- Measurement of these functions is not quite clear from the description of the respective functions.

- The drying process that uses internal heating like microwaves is not considered in this model. Therefore, it is not clear as to whether other drying methods, as opposed air-

drying, are suitable for using this model. As a result, it becomes less generic for different types of drying.

3   Key challenges of the existing models

Extensive review of the empirical and theoretical models of porosity prediction revealed that reliable porosity prediction during drying process still needs further attention of the researchers. A central issue is that there is no generic model that can be applied to different products and drying processes. Literature confirms that both product type and drying technology discernibly affect pore formation and the pore evolution during drying of food materials. In order to adapt the material properties, the previous studies mainly considered the structural parameters like the volumetric shrinkage coefficient, shrinkage-expansion coefficient and shrinkage-collapse coefficient. Most of these properties vary with the product types and the drying conditions.

The measurement of the structural parameters means that there is a necessity for experimental data. A generic theoretical model of porosity should avoid these structural parameters, which vary in drying conditions. A model containing parameters that are not influenced by the drying conditions can be treated as generic model.

The changes in porosity in food materials over the period of drying mainly depend on volume change and void formation due to water migration. Both can occur simultaneously, depending on the material properties and drying conditions. The following are the important factors that must be taken into consideration for porosity prediction:

- Drying time is a vital factor that influences the collapse of cells during the course of drying. For example, lower drying temperatures (i.e. longer drying time) can cause structural damage to the food product. As most of the food materials have a rubbery state, the instantaneous material temperature remains above the glass transition temperature during drying (these temperatures are explained in the next point) (Joardder, Kumar, & Karim, 2017b). Longer drying time causes the collapse of the

plant tissue, even when drying at a low temperature, as the plant tissue has very low glass transition temperature (Karathanos et al., 1993).

- Process parameters are found as the key dominator of structural changes in food materials over the period of drying. In particular, greater differences between material and glass transition temperatures ($T-T_g$), more the collapse is. During drying, the glass transition temperature (T_g) is the critical temperature at which the material changes its conditions from 'glassy' to 'rubbery'. Plant-based food sample transforms to rubbery state from glassy state because of the migration of water and sample temperature exceed the glass transition temperature

- Material properties play a vital role in the retention of the fresh like material structure as they resist the external forces from heat and mass transfer. Basic material properties do not change with the variation of drying conditions (Khan, Wellard, Nagy, Joardder, & Karim, 2017). Water content and water distribution are such parameters that can be taken into consideration in this regard.

4   Improved understanding of pore evolution during drying

Even though porosity development is mainly attributed to the void spaces created by migrated water, the shrinkage of solid matrix towards the centre of the sample compensates the void volume. Therefore, the insight of the heat and mass transfer mechanisms, as well as the structural deformation is essential to understand the evolution of porosity in the course of the drying. These transfer mechanisms and structural changes are significantly influenced by both material properties and process parameters. Materials properties like moisture content, solid density, initial density, particle density and glass transition temperature are the important properties that should be taken into consideration. The air temperature is the prime process factor that significantly influences the structural modification of the food material. An improved

interpretation of pore formation and evolution considering these material properties and process conditions is discussed in the following sections.

4.1 Water distribution inside the food

As the solid food matrix is hygroscopic (Joardder et al., 2017a; Rahman & Joardder M. U.H., 2016) the bulk moisture removal assumption cannot explain the characteristics of porosity. Pore formation is prevented by shrinkage, collapse, and expansion of food material during drying. Water in food materials can be classified as free water and bound water. While it can also be classified by the spatial position of the water is either intercellular, intracellular or within the cell wall (Joardder, Kumar, Brown, & Karim, 2015a; Joardder, Kumar, & Karim, 2013) as shown in Figure 3.

Water inside the cell is known as intracellular water while intercellular water is the water that is present in capillaries. Intracellular water varies between 78-97% in different fruits and vegetables (Khan et al., 2017), with the rest being intercellular. It is hard to determine the proportion of water within the cell and cell wall (Joardder et al., 2015a).

4.2 Water pathways during drying

Different pathways for water flux were observed depending upon the food structure, food composition and drying conditions (Joardder et al., 2017a). Considering this, a conceptual map is developed by the current authors, showing the different pathways of water migration in plant tissue (Figure 4).

The figure shows that water can migrate through different pathways from different spaces in the food tissue. For example, water from the cell migrates through cell walls (including cell membranes) into the intercellular space, then it moves into the atmosphere (Rahman & Joardder M. U.H., 2016). When rupture occurs due to higher drying temperature, a percentage of the water directly travels into the tissue while the rest of it migrates into the atmosphere through the intercellular space. The water in the cell wall requires relatively high energy for migration as it

needs to pass through inter-microfibrillar spaces (Joardder, Kumar, Brown, & Karim, 2015b; Lewicki & Lenart, 1995).

Apart from the pathways mentioned above, phase change patterns (from liquid water to vapour) are important considerations in the prediction of structural changes during drying.

4.3   Phase change (liquid water to vapour)

Moisture flux is a rate measurement that refers how fast the moisture is migrating across a defined cross section. The total flux of moisture is the summation of liquid water and vapour fluxes as shown in Figure 5. Both of the fluxes are results of gas pressure gradient (convective flux) and capillary pressure gradient (diffusive flux).

A decreasing trend of liquid flux is found during drying time. The highest liquid flux exists where the moisture gradient shows higher. Moreover, from the literature, it is found that almost 90% of total water migrate as a liquid. On the other hand, water vapour flux is increased over the time of drying, and the maximum total vapour flux is located at the surface of the sample due to the significant concentration gradient between the vapour at the surface and the ambient air. Moreover, the vapour flux decreases to the direction of core region because of the lower molecular diffusivity of vapour water. Due to the hygroscopic nature of food material, the convective flux of both liquid and vapour water is almost insignificant. Therefore, diffusive flux dominates over the convective flux throughout the food processing time.

Evaporation rate is highly dependent on temperature and pressure gradient. Furthermore, the liquid water saturation becomes lower near the surface of the sample thus the vapour pressure, and equilibrium vapour pressure becomes similar. In addition to this, the rate of evaporation needs to be controlled in order to minimise the surface fracture. Tanaka (2012) proposes that controlling evaporation rate can be the way of minimising surface crack formation.

Putting all of this together, the types of flux and evaporation rate significantly affect the formation and modification of food structure. Consideration of these in pore formation model would enhance the insight of the structural modification over the time of drying.

4.4 Solid mobility temperature as a process parameter

The temperature at (or above) which the amorphous material changes from a glassy to rubbery state is called glass transition temperature (T_g) (Champion, Le Meste, & Simatos, 2000). In glassy state, the material matrix has a very high viscosity, in the range of 10^{12} to 10^{13} Pa s. When the matrix behaves like a solid, it can retain the rigidity of its structure by supporting its body weight against the force of gravity (Angell, 1988; Lewicki, 1998). Therefore, $\Delta T = T - T_g$ can be treated as the driving force of structural collapse (Del Valle et al., 1998), where T is the temperature of the sample undergoing drying. In this paper, *mobility temperature* will be used to refer ΔT .

Effect of glass transition temperature on the rate of shrinkage is presented in Figure 6 (developed by current authors) and is explained below.

- The rate of shrinkage is closely related to its physical state (Levi & Karel, 1995). When the material is in a rubbery state, it has a high mobility within the matrix. On the other hand, is has a low mobility when the material is in the glassy state. Volume shrinkage compensates almost the all the air volume increased due to water migration (Achanta & Okos, 1996).

- Shrinkage characteristics depend greatly on the value of mobility temperature. The high rate of shrinkage is caused due to a high mobility temperature, which can be observed in the early stage of drying. As drying progresses, the mobility temperature decreases and the shrinkage rate sharply declines due to the increase of collapse resistance in the dried material (Karathanos et al., 1993; Katekawaa & Silvaa, 2007).

- The sample shrinks until the mobility temperature reaches zero or close to zero. So drying at higher temperature causes shrinkage even with very low moisture content (Kurozawa, Hubinger, & Park, 2012).

4.5 A better approach of describing the pore formation during drying

The plant tissue undergoes stresses during shrinkage and deformation because of simultaneous thermal and moisture gradients. The stresses generated by the moisture gradient takes place during almost the entire drying period, while the thermal stress is more remarkable in the earlier stages of drying (Jayaraman, Gupta, & Rao, 1990; Lewicki & Pawlak 2003). Therefore, the stress generated by the moisture gradient is the dominant contributor of plant tissue shrinkage during drying.

Based on microstructure studies and water migration analysis conducted by the authors, pore formation mechanism has been presented in Figure 7, and a step by step description is provided below:

I. At the very initial stage of the drying process, only intercellular water migrates from the tissues, but this does not cause any noticeable shrinkage of the sample.

II. After migration of the intercellular water (known as a falling rate stage of drying), the intracellular water starts migrating from the cells and causes shrinkage of initial pores. Also, the early stage of intracellular water migration, volumetric shrinkage is much more closely correlated to the amount of removed water.

III. Cell shrinkage occurs due to a lower turgor pressure. This is caused due to the migration of large amounts of cell water. It is vital to predicting the proportion of shrinkage of the sample with the migration of water in this stage. One of the possible solutions may be the determination of the ratio of the densities, particularly the ratio of water density and particle density. In other words, the shrinkage compensates for the void developed due to

water migration, depends on the particle density of the sample. It is hypothesised that, if the ratio is unity there will be complete shrinkage.

In the initial stages, food material encounters shrinkage without cell collapse. However, cell breakage is observed as the drying time increases. This does not, however, severely collapse the cell. Cell collapse occurs only during cell wall water migration. Parenchyma cells in plant tissue, as shown in Figure 6, are typically thin-walled and abundant. Vacuoles that serve as cell water storage containers are located inside these cells. Vascular solutes are usually osmotically active, which push against the cell membrane lining the cell wall. The turgor pressure develops and keeps the cells in a state of elastic stress, thus maintaining the shape and tension in the tissue (Ilker & Szczesniak, 1990). If the turgor pressure is lost, the structure of the fruit collapses, and once this occurs, it cannot be reversed (Reeve, 1970).

IV. Pore expansion occurs in the later stage of drying when the food matrix becomes sufficiently dry and increases in viscosity (Del Valle et al., 1998), thus hindering both shrinkage and collapse (Karathanos, Anglea, & Karel, 1996a). In addition to this, further drying also causes enlargement of the intercellular space. The cell wall and solid matrices of the plant based cellular tissues are flexible enough to allow migration of water from the vacuole, allowing shrinkage of the entire tissue but not increasing the volume of the intercellular spaces (Hills & Remigereau, 1997).

Some of the possible sequences of zero shrinkage, partial shrinkage and collapse of food structure are shown in Figure 6, although there could be many other possibilities. Due to the diverse nature of the different plant tissues, it is challenging to accommodate all of the physics involved in pore formation and evolution over the period of drying. In addition to this, some of the other variables and outcomes including, case hardening and anisotropic shrinkage are not taken into consideration.

5   Conclusion

A generic model for predicting porosity of food materials is complex due to its dependence on many interrelated variables. Some of these include its hygroscopic amorphous porous structure and simultaneous heat and mass transfer facilitating multiphase composition and phase change. A generic model needs to be able to predict the porosity of any food product during drying regardless of the process. Although extensive research has been carried out on pore formation, no study exists that considers both process conditions and material properties. All the theoretical models proposed in the literature consist of at least one structural deformation coefficient of empirical nature. In this study, some vital factors were identified for formulating a theoretical model of pore formation and evolution during drying. The comprehensive understanding of the prediction of the pore formation mechanism needs to be researched further. A wider variety of processing conditions and various food properties needs to be considered in the future research to develop a realistic and generic model of pore formation. The author's research group continues to work toward this goal hopefully will come up with an exact generic porosity model.

Nomenclature

Nomenclature	Meanings	Unit
M	Mass	Kg
V	Total Volume	m^3
W	Water content	Kg of water/kg of sample

X	Water content	Kg of water/kg of solid
T	Temperature	K
M	Molecular weight of water	kg/mole
a, b, c, d, e, f, j	Fitting parameters involved in empirical models	
Greek symbols		
φ	Shrinkage expansion function	
ε	Porosity	
δ	Collapse function	
ρ	Density	kg/m^3
β	Density ratio, volume shrinkage coefficient	
ϕ, δ	Volume-shrinkage coefficient	
Subscripts		
0	Initial	
A	Air	
B	Bulk	
S	Solid	
W	Water	
P	Particle	
G	Glass transition	
M	Material	

6 References

Achanta, S., & Okos, M. R. (1996). Predicting the quality of dehydrated foods and biopolymers - research needs and opportunities. Drying Technology, 14(6), 1329-1368.

Angell, C. A. (1988). Perspective on the glass transition. *Physics and Chemistry of Solids, 49*, 863–871.

Ayrosa, A. M. I. B., & Pitombo, R. N. M. (2003). Influence of plate temperature and mode of rehydration on textural parameters of precooked freeze-dried beef. *Journal of Food Processing and Preservation, 27*(3), 173–180.

Bai, Y., Rahman, M. S., Perera, C. O., Smith, B., & Melton, L. C. (2001). State diagram of apple slices: Glass transition and freezing curves. *Food Research International, 34*, 89-95.

Bhatnagar, S., & Hanna, M. A. (1997). Modification of microstructure of starch extruded with selected lipids. *Starch/Staerke, 49*(1), 12-20.

Champion, D., Le Meste, M., & Simatos, D. (2000). Towards an improved understanding of glass transition and relaxations in foods: molecular mobility in the glass transition range. *Trends in Food Science & Technology, 11*(2), 41-55. doi: 10.1016/S0924-2244(00)00047-9

Datta, A. K. (2007). Porous media approaches to studying simultaneous heat and mass transfer in food processes. II: Property data and representative results. *Journal of Food Engineering, 80*(1), 96-110.

de Kruif, C. G. (2012). Concluding remarks: the future of soft matter and food structure. *Faraday Discussions, 158*(0), 523-527. doi: 10.1039/C2FD20122D

Del Valle, J. M., Cuadros, T. R. M., & Aguilera, J. M. (1998). Glass transitions and shrinkage during drying and storage of osmosed apple pieces. *Food Research International, 31*(3), 191–204.

Hills, B. P., & Remigereau, B. (1997). NMR studies of changes in subcellular water compartmentation in parenchyma apple tissue during. *International Journal of Food Science & Technology, 32*(1), 51.

Huang, C. T., & Clayton, J. T. (1990). Relationships between mechanical properties and microstructure of porous foods: Part I. A review. *Engineering of food. Vol. 1. Physical properties and process control, 1*, 352-360.

Hussain, M. A., & Rahman, M. S. (1999). Thermal conductivity prediction of fruits and vegetables using neural networks. . *International Journal of Food Properties, 2*(2), 121-137.

Hussain, M. A., Shafiur Rahman, M., & Ng, C. W. (2002). Prediction of pores formation (porosity) in foods during drying: Generic models by the use of hybrid neural network. *Journal of Food Engineering, 51*(3), 239-248. doi: 10.1016/s0260-8774(01)00063-2

Hutchinson, R. J., Siodlak, G. D. E., & Smith, A. C. J. (1987). Influence of processing variables on the mechanical properties of extruded Maize. *Journal of Material Science, 22*, 3956–3962.

Ilker, R., & Szczesniak, A. S. (1990). Structural and chemical bases for texture of plant foodstuffs. *Journal of Texture Studies, 21*(1), 1-36. doi: 10.1111/j.1745-4603.1990.tb00462.x

Jayaraman, K. S., Gupta, D. K. D., & Rao, N. B. (1990). Effect of pretreatment with salt and sucrose on the quality and stability of dehydrated cauliflower. *International Journal of Food Science & Technology, 25*(1), 47-60. doi: 10.1111/j.1365-2621.1990.tb01058.x

Joardder, M. U. H., Kumar, C., Brown, R. J., & Karim, M. A. (2015a). Effect of cell wall properties on porosity and shrinkage of dried apple. *International Journal of Food Properties, In Press*.

Joardder, M. U. H., Kumar, C., Brown, R. J., & Karim, M. A. (2015b). A micro-level investigation of the solid displacement method for porosity determination of dried food. *Journal of Food Engineering, 166*, 156-164. doi: http://dx.doi.org/10.1016/j.jfoodeng.2015.05.034

Joardder, M. U. H., Kumar, C., & Karim, M. A. (2013, 1-3 November). *Better understanding of food material on the basis of water distribution using thermogravimetric analysis* . Paper presented at the International Conference on Mechanical, Industrial and Materials Engineering, Rajshahi, Bangladesh.

Joardder, M. U. H., Kumar, C., & Karim, M. A. (2017a). Food structure: Its formation and relationships with other properties. *Critical Reviews in Food Science and Nutrition, 57*(6), 1190-1205. doi: 10.1080/10408398.2014.971354

Joardder, M. U. H., Kumar, C., & Karim, M. A. (2017b). Multiphase transfer model for intermittent microwave-convective drying of food: Considering shrinkage and pore evolution. *International Journal of Multiphase Flow, 95*, 101-119. doi: https://doi.org/10.1016/j.ijmultiphaseflow.2017.03.018

Karathanos, V., Anglea, S., & Karel, M. (1993). Collapse of structure during drying of celery. *Drying Technology, 11*(5), 1005-1023.

Karathanos, V. T., Anglea, S. A., & Karel, M. (1996a). Structural collapse of plant materials during freeze-drying. *Journal of Thermal Analysis, 47*(5), 1451-1461.

Karathanos, V. T., Kanellopoulos, N. K., & Belessiotis, V. G. (1996b). Development of porous structure during air drying of agricultural plant products. *Journal of Food Engineering, 29*(2), 167-183.

Karunasena, H. C. P., Senadeera, W., Brown, R. J., & Gu, Y. T. (2014). A particle based model to simulate microscale morphological changes of plant tissues during drying. *Soft Matter, 10*(29), 5249-5268. doi: 10.1039/C4SM00526K

Katekawa, M. E. a. S., M.A.;. (2004, 22-25 August 2004). *Study of porosity behaviour in convective drying of bananas.* Paper presented at the Drying 2004 – Proceedings of the 14th International Drying Symposium (IDS 2004), São Paulo, Brazil.

Katekawaa, M. E., & Silvaa, M. A. (2007). On the influence of glass transition on shrinkage in convective drying of fruits: A case study of banana drying. *Drying Technology: An International Journal, 25*(10), 1659-1666.

Khalloufi, S., Almeida-Rivera, C. and Bongers, P.;. (2009). A theoretical model and its experimental validation to predict the porosity as a function of shrinkage and collapse phenomena during drying. *Food Research International, 42*(8), 1122-1130. doi: 10.1016/j.foodres.2009.05.013

Khan, M. I. H., Wellard, R. M., Nagy, S. A., Joardder, M. U. H., & Karim, M. A. (2017). Experimental investigation of bound and free water transport process during drying of hygroscopic food material. *International Journal of Thermal Sciences, 117*, 266-273. doi: http://doi.org/10.1016/j.ijthermalsci.2017.04.006

Kilpatric, P. W., Lowe, E., & Van Arsdel, W. B. (1955). *Tunnel dehydrators for fruits and vegetables.* New York: Academic Press.

Krokida, M. K., & Maroulis, Z. B. (1997). Effect of drying method on shrinkage and porosity. *Drying Technology, 15*(10), 2441–2458.

Krokida, M. K., Zogzas, N. P., & Maroulis, Z. B. (1997). Modelling shrinkage and porosity during vacuum dehydration. *International Journal of Food Science & Technology, 32*(6), 445-458. doi: 10.1111/j.1365-2621.1997.tb02119.x

Kurozawa, L. E., Hubinger, M. D., & Park, K. J. (2012). Glass transition phenomenon on shrinkage of papaya during convective drying. *Journal of Food Engineering, 108*(1), 43-50. doi: 10.1016/j.jfoodeng.2011.07.033

Levi, G., & Karel, M. (1995). Volumetric shrinkage (collapse) in freeze-dried carbohydrates above their glass transition temperature. *Food Research International, 28*(2), 145-151. doi: 10.1016/0963-9969(95)90798-F

Lewicki, P. P. (1998). Some remarks on rehydration properties of dried foods. *Journal of Food Engineering, 36*, 81–87.

Lewicki, P. P., & Lenart, A. (Eds.). (1995). *Osmotic Dehydration of fruits and vegetables* (Vol. 1). New York: Marcel Dekker.

Lewicki, P. P., & Pawlak , G. (2003). Effect of drying on microstructure of plant tissue. *Drying Technology, 21*(4), 657-683.

Liu, X., Chen, J. , Liu, M., Li, Z., Tao, Y., Zhu, D. . (2010). *The effect of biological material's tissue shrinking on moisture diffusivity during hot-air-drying.* Paper presented at the World Automation Congress (WAC), 2010, Kobe.

Lozano, J. E., Rotstein, E., & Urbicain, M. J. (1980). Total porosity and open-pore porosity in the drying of fruits. *Journal of Food Science, 45*, 1403-1407.

Lozano, J. E., Rotstein, E., & Urbicain, M. J. (1983). Shrinkage, porosity and bulk density of foodstuffs at changing moisture contents. *Journal of Food Science, 51*, 113-120.

Madamba, P. S., Driscoll, R. H., & Buckle, K. A. (1994). Shrinkage, density and porosity of garlic during drying. *Journal of Food Engineering, 23*(3), 309-319.

Marousis, S. N., & Saravacos, G. D. (1990). Density and Porosity in Drying Starch Materials. *Journal of Food Science, 55*(5), 1367-1372. doi: 10.1111/j.1365-2621.1990.tb03939.x

Miles, C. A., Beck, G. V., & & Veerkamp, C. H. (1983). *Calculation of thermophysical propcrties of foods*. London: Applied Science Publishers.

Perez, M. G. R., & Calvelo, A. (1984). Modeling the thermal-conductivity of cooked meat. *Journal of Food Science, 49*(1), 152-156.

Prothon, F., Ahrné, L., & Sjöholm, I. (2003). Mechanisms and Prevention of Plant Tissue Collapse during Dehydration: A Critical Review. *Critical Reviews in Food Science and Nutrition, 43*(4), 447-479.

Rahman, M. M., & Joardder M. U.H., K., M.A. (2016). *Investigation of cellular level water in plant-based food material.* Paper presented at the 20th Internatonal Drying Symposium, Gifu, Japan.

Rahman, M. S. (2001). Towards prediction of porosity in food foods during drying: A brief review. *Drying Technology, 19*(1), 3-15.

Rahman, M. S., Perera, C. O., Chen, X. D., Driscoll, R. H., & Potluri, P. L. (1996). Density, shrinkage and porosity of calamari mantle meat during air drying in a cabinet dryer as a function of water content. *Journal of Food Engineering, 30*(1-2), 135-145.

Rapusas, R. S., & Driscoll, R. H. (1995). Thermophysical properties of fresh and dried white onion slices. *Journal of Food Engineering, 24*(2), 149-164.

Reeve, R. M. (1970). Relationships of histological structure to texture of fresh and processed fruits and vegetables. *Journal of Texture Studies, 1*(3), 247-284. doi: 10.1111/j.1745-4603.1970.tb00730.x

Sablani, S. S., Rahman, M. S., Al-Kuseibi, M. K., Al-Habsi, N. A., H., A.-B. R., Al-Marhubi, I., & Al-Amri, I. S. (2007). Influence of shelf temperature on pore formation in garlic during freeze-drying. *Journal of Food Engineering, 80*(1), 68-79. doi: 10.1016/j.jfoodeng.2006.05.010

Santos, P. H. S., & Silva, M. A. (2008). Retention of Vitamin C in Drying Processes of Fruits and Vegetables—A Review. *Drying Technology, 26*(12), 1421-1437. doi: 10.1080/07373930802458911

Shafiur Rahman, M. (2003). A theoretical model to predict the formation of pores in foods during drying. *International Journal of Food Properties, 6*(1), 61-72. doi: 10.1081/jfp-120016624

Tanaka, H. (2012). Viscoelastic phase separation in soft matter and foods. *Faraday Discussions, 158*(0), 371-406. doi: 10.1039/C2FD20028G

van der Sman, R. G. M., & van der Goot, A. J. (2009). The science of food structuring. *Soft Matter, 5*(3), 501-510. doi: 10.1039/B718952B

Vincent, J. F. V. (1989). Relationship between density and stiffness of apple flesh. *Journal of the Science of Food and Agriculture, 47*(4), 443-462. doi: 10.1002/jsfa.2740470406

Xiong, X., Narsimhan, G., & Okos, M. R. (1992). Effect of composition and pore structure on binding energy and effective diffusivity of moisture in porous food. *Journal of Food Engineering, 15*(3), 187-208.

Zogzas, N. P., Maroulis, Z. B., & Marinos-Kouris, D. (1994). Densities, shrinkage and porosity of some vegetables during air drying. *Drying Technology, 12*(7), 1653-1666.

Table 1. Summary of empirical models predicting porosity during drying

References	7 Empirical Equation	Drying condition	Food item	R^2
Lozano et al.[1]	$\varepsilon = Y \dfrac{a - b\exp(cX)}{d\exp(eX) - f\exp(jX)}$	Air Drying (60^0 C)	Apple	0.97
Mattea et al.[2]	$\varepsilon = Y \dfrac{X - a}{(X - a) + \dfrac{b}{c - X}}$	Air drying, 55^0C	Apple, pears, Potato	N/A
Rahman et al.[3]	$\varepsilon = a + b\left[\dfrac{W}{W_0}\right]$	Air Drying, (70^0C)	Squid	0.97
Modamba et al.[4]	$\varepsilon = a + bW + cW^2$	Air drying (70^0C)	Garlic	N/A
Joshi et al.[5]	$\varepsilon = a + bX$	Air Drying (47^0C)	Pumpkin Seed	0.988
Rapusas et al.[6]	$\varepsilon = a + bW + cW^3$	Air Drying (70^0C)	Onion	0.974
Rahman et al.[7]	$\varepsilon = a + b\left[\dfrac{W}{W_0}\right] + c\left[\dfrac{W}{W_0}\right]^2$	Air Drying (70^0C)	Calamari Mantle Meat	N/A
Magee et al. [8]	$\varepsilon = a + b\,exp\left[\dfrac{X}{c}\right]$	Air Drying 30, 45, 60^0C Air velocity: 3m/s	Potato	0.998

Guine et al.[9]	$\varepsilon = \dfrac{a}{1+bX}$	Air and Solar Drying	Pear	N/A
Rahman et al.[10]	$\varepsilon = a + bX + cX^2$	Air Drying (50,80,105^{0}C)	Apple	0.93-0.97
Katekawa et al.[11]	$\varepsilon = \left(a + b \left(ln\dfrac{X}{X_0} \right)^2 \right)^{0.5}$	Air Drying (40,50^{0}C)	Banana	N/A
Perez et al.[12]	$\varepsilon = a\left(W_0 - W\right)^b$	Thermal conduction	Meat	N/A

Table 2: Summary of the porosity prediction model using hybrid neural networks

Inputs	Porosity expression	Absolute mean percent error
Temperature, water content	$\varepsilon = 0.5X_w^2 - 0.8X_w - 0.002T^2 + 0.02T - 0.15$	56.5
Temperature, water content, initial porosity	$\varepsilon = 0.5X_w^2 - 0.8X_w - 0.002T^2 + 0.02T - 0.15(1-\varepsilon_0)$	0.98
Temperature, water content, initial porosity, product type	$\varepsilon = 0.5X_w^2 - 0.8X_w - 0.002T^2 + 0.02T - 0.05(1-\varepsilon_0)F$	0.58

Table 3.Summery of implementation of Zogzas et al. [13] porosity model

References	Drying Technology	Drying conditions	Food stuff
Zogas et al.[13]	Air Drying	Drying air temperature: 70^0C Air velocity: 2.5 m/s Relative humidity: 20%, 30%, 45% and 60%	Carrot, Apple Potato
Krokida et al. [14, 15]	Air Drying	Drying temperature: 70^0 Relative humidity: 7%	Banana Apple Carrot Potato
	Vacuum Drying	Drying temperature:70^0 Relative humidity: 7% Vacuumed pressure: 33 mbar	
	Microwave Drying	Microwave power: 810 W	
	Freeze drying	Drying temperature: -35 ^{0}C	
	Osmotic dehydration+ Air Drying	50% sugar Drying temperature: 40^0 C Drying time: 24 hours	
Krokida et al. [16]	Air Drying	Drying temperature:70^0 Relative humidity: 7%	Banana Apple Carrot
	Microwave drying + air drying	Microwave drying	

		continues 1.5 min	Potato
	Microwave – vacuum drying + Air drying	Microwave drying continues 1.5 min and vacuum at 15 mmHg	
Tsami et al. [17]	Air drying	Drying temperature: 50, 60 and 70 ^{0}C Air velocity: 3.5 m/s Relative humidity: 15%	Quince, Prune, Fig, Strawberry, Avocado
Guine et al.[9]	Solar Drying	Drying temperature: 15-45^{0}C Drying time: 264 hours	Pear
	Air drying	Air flow rate: 300m^3/h	
Mayor et al.[18]	Osmotic + Air Drying	Drying temperature: 70^{0}C Relative humidity: 6$\pm$2%	Pumpkin
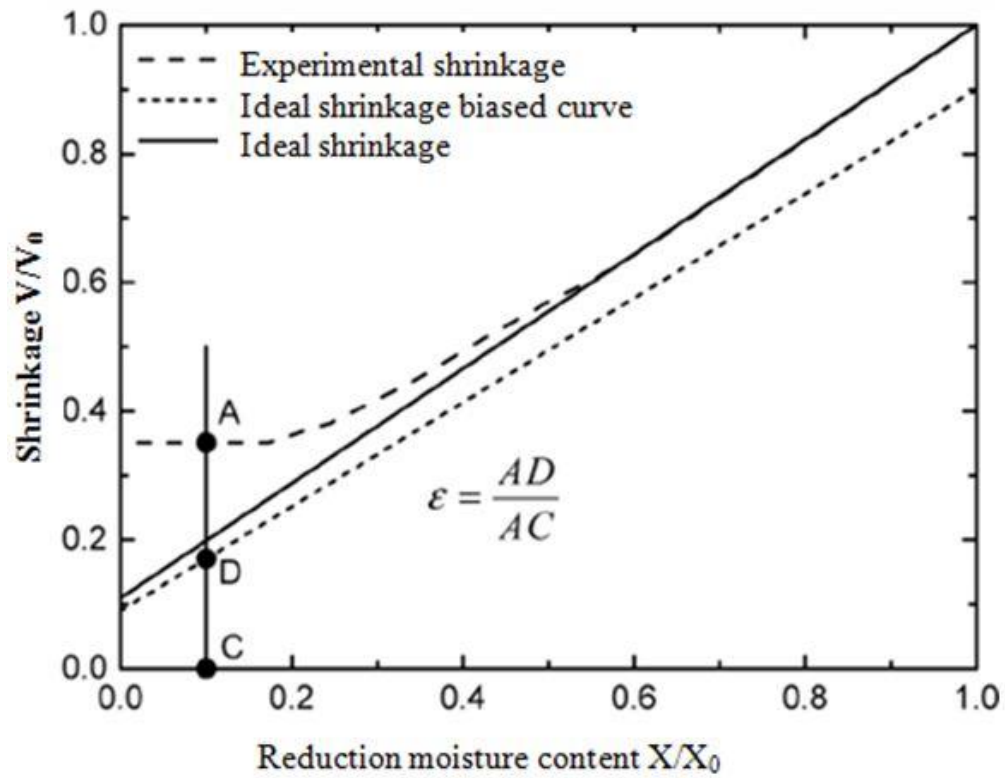
Figure 1. Non-ideal shrinkage curve with initial porosity: ideal shrinkage curve (plain line); ideal shrinkage biased curve, taking initial porosity into account (small dots) and the experimental curve (dashes). Adapted from (Madiouli, et al., 2007)
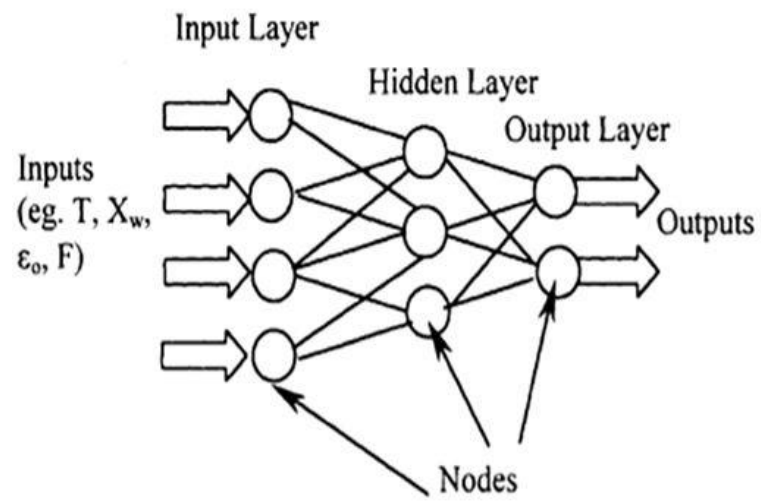
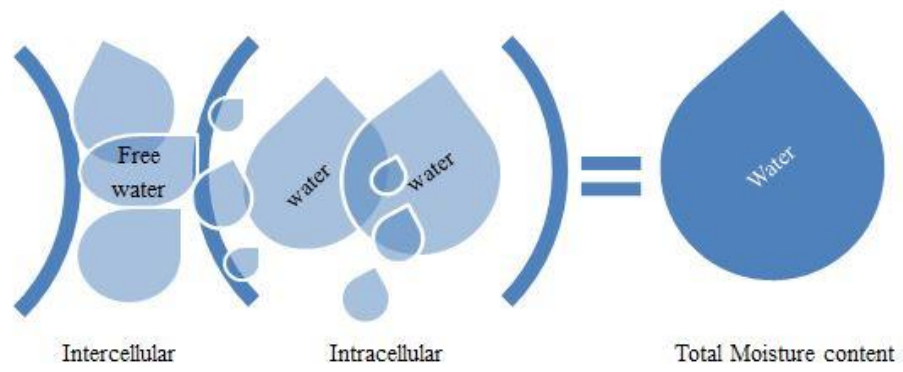Figure 2: Multi-layer perception network for the hybrid neural network.

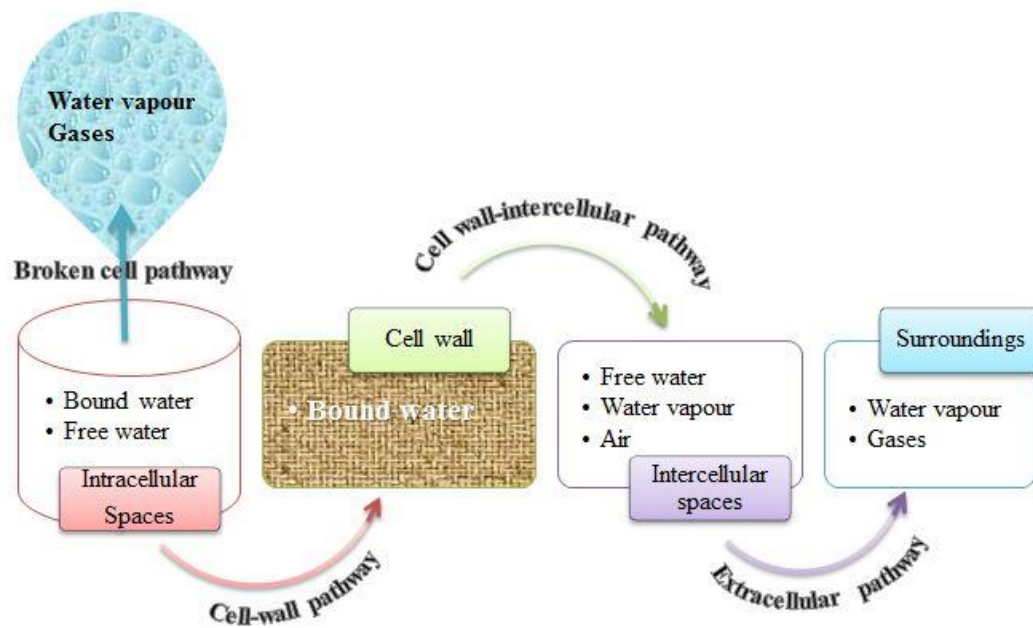Figure 3. Different type of the water inside the plant based food materials

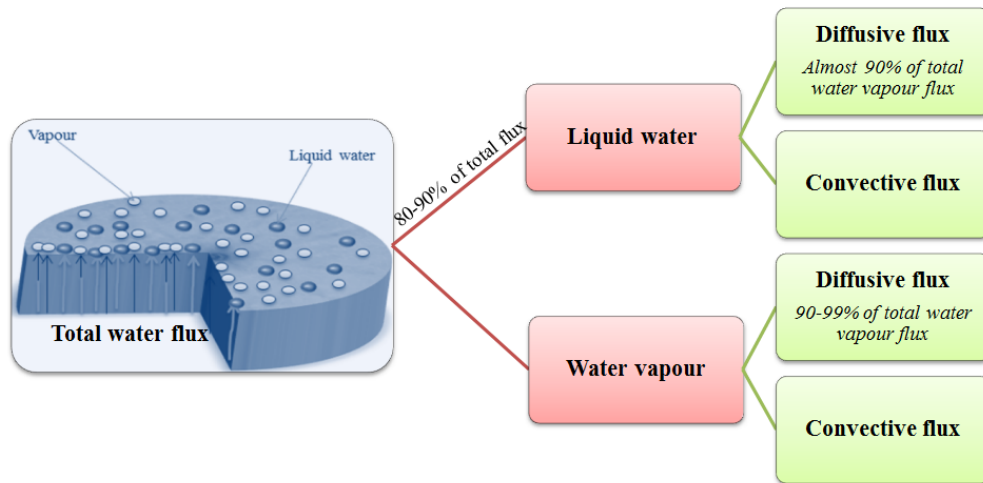Figure 4. Conceptual map of different pathways of water migration in plant tissue

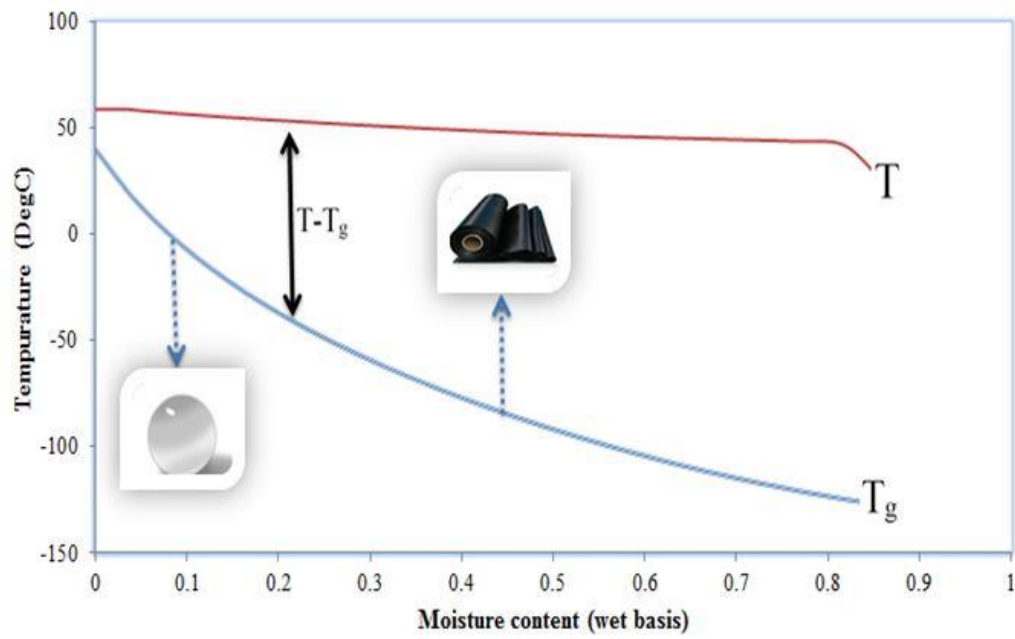Figure 5. Phase change strategy of moisture of food material during drying
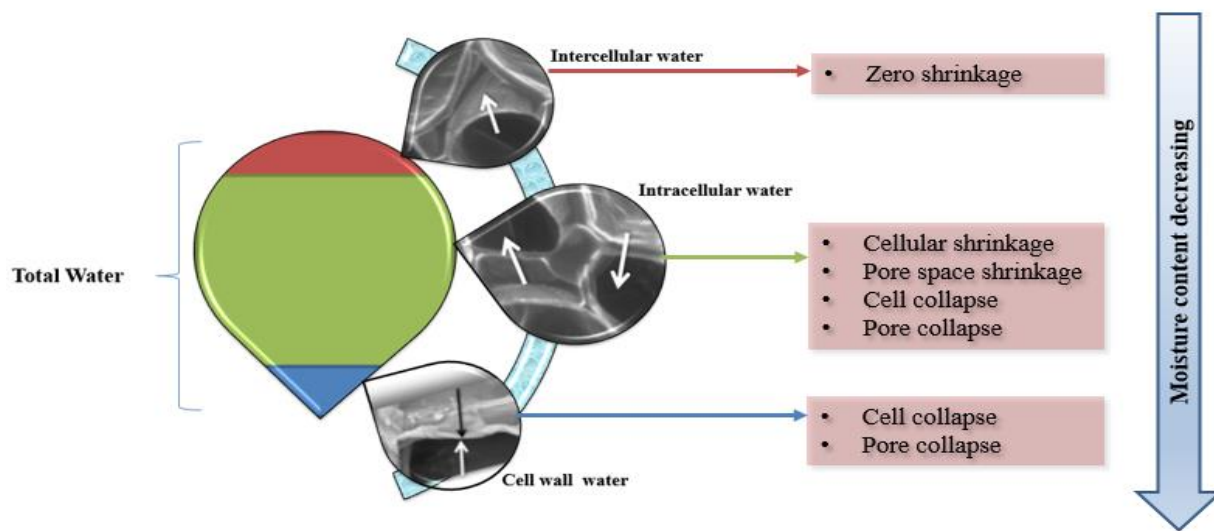
Figure 6. Effect of glass transition temperature on plant tissue

Figure 7. Physical interpretation of pore evolution over the time of drying and moisture content